



Can pollen affect precipitation?

Marje Prank¹, Juha Tonttila^{2,3}, Xiaoxia Shang², Sami Romakkaniemi², Tomi Raatikainen¹

¹Climate System Research Unit, Finnish Meteorological Institute, Helsinki, 00560, Finland

²Atmospheric Research Centre of Eastern Finland, Finnish Meteorological Institute, Kuopio, 70211, Finland

³CSC - IT Center for Science Ltd., Espoo, 02101, Finland

Correspondence to: Marje Prank (marje.prank@fmi.fi)

Abstract. Large primary bioparticles such as pollen can be abundant in the atmosphere, for example near surface pollen concentrations above 10 000 particles per cubic meter can occur during intense pollination periods. On one hand, due to their large size (10-100 micrometres), pollens can act as giant cloud condensation nuclei and enhance the collision-coalescence process in clouds that leads to drizzle formation. On the other hand, in humid conditions pollens are known to rupture and release many fine particles that can increase the cloud stability by reducing the droplet size. Additionally, both whole pollen grains and the sub-pollen particles released by pollen rupture are known to act as ice-nucleating particles (INPs). Due to these complex interactions, the role of pollen in modulating the cloud cover and precipitation remains uncertain.

We used the UCLALES-SALSA large eddy simulator for simulating birch pollen effects on liquid and mixed-phase clouds. Our simulations show that the pollen concentrations observed during the most intense pollination seasons can locally enhance precipitation from both liquid and mixed phase clouds, while more commonly encountered pollen concentrations are unlikely to cause a noticeable change. The liquid precipitation enhancement depended linearly on the emitted pollen flux in both liquid and mixed phase clouds, however, the slope of this relationship was case dependent. Ice nucleation happened at relevant degree only if the process of rupturing pollens producing large number of fine ice nucleating particles was included in the simulations. The resulting precipitation saturated for the highest INP concentrations. Secondary ice formation by rime splintering had only minor effect in the considered one-day timescale.



1 Introduction

25 Large primary biological aerosol particles (PBAPs) such as pollen can be abundant in the atmosphere. For instance, according
to Ranta and Satri (2007), the daily mean concentrations of birch plus alder pollen in Finland can exceed 1 000 pollen/m³ for
up to 2 weeks per year. Daily mean concentrations above 10 000 pollen/m³ occur during intense pollination periods - in United
States such pollen concentrations from both deciduous and evergreen trees have been observed (Steiner et al., 2015) and
bihourly concentrations exceeding 50 000 birch pollen/m³ were observed in Vehmasmäki station in Finland in May 2021. In
30 the current study we concentrate mostly on birch pollen as one of the most abundant pollens in boreal and northern temperate
climates of Northern Hemisphere, such as Central and Northern Europe (Skjøth et al., 2013) or North America (Steiner et al.,
2015). Birch pollen is also well studied due to its high allergenicity. The abundance of pollen in many tree species including
birch and alder varies between years depending on weather conditions and flowering intensity of previous year (Dahl et al.,
2013). Pollen concentrations also exhibit regular diurnal variations with afternoon peaks, although Rantio-Lehtimäki et al.
35 (1991) found the concentrations of tree pollen to stay relatively constant over the day, with slight minimum in early morning.
Due to their large size (10-100 micrometres in diameter), pollens can act as giant cloud condensation nuclei (GCCN) and
enhance the collision-coalescence process in clouds that leads to drizzle formation (Houghton, 1938). In humid conditions
pollens are known to rupture and release a large number of fine sub-pollen particles (SPPs) (Emmerson et al., 2021; Stone et
al., 2021; Suphioglu et al., 1992; Taylor et al., 2004; Wozniak et al., 2018). In mixed phase clouds both pollen and SPPs can
40 also act as ice nucleating particles (INPs). Pollens of spring flowering trees such as birch and alder have been shown to be
good ice nucleators in relatively higher temperatures (Dreischmeier et al., 2017; Gute and Abbatt, 2020). On the other hand,
these SPPs acting as extra CCN can increase the cloud stability by reducing the droplet size.

The processes leading to pollen rupture are not well understood. While sub-pollen particles from birch pollen have been
observed both in lab and in atmosphere (Burkart et al., 2021; Rantio-Lehtimäki et al., 1994; Schäppi et al., 1997), the frequency
45 of this process happening in atmosphere has not been quantified. More research exists about grass pollen related to asthma
outbreaks coinciding with thunderstorms, but conditions leading to it have not been well quantified (Emmerson et al., 2021).
The only data available to our knowledge regarding pollen rupture due to high air humidity was collected by Zhou (2014) for
wheat and pine pollens. Wheat pollen was the only one rupturing in their setup. Unfortunately, they made no experiments with
birch pollen. Large uncertainties exist also in the number of SPPs released from a rupturing birch pollen and their size
50 distribution.

Large spread exists also in the measurements of ice nucleation efficiency by pollen and SPPs. The median freezing
temperatures gathered and measured for birch pollen reach from -13.4 to -27 °C and for alder from -7.3 to -17 °C and are
sensitive to atmospheric processing experienced by the pollen grains (Gute et al., 2020; Gute and Abbatt, 2020). The
temperature of freezing onset is challenging to measure and uncertain (Duan et al., 2023).

55 Small number of global and regional modelling studies have investigated the impact of pollen and SPPs to precipitation (e.g.
Werchner et al., 2022; Wozniak et al., 2018; Zhang et al., 2024). However, often the pollen concentrations in those are low,



representative of long-time or large-scale averages, while during intense flowering on most years the concentrations can locally reach many times what is used in those studies. Also, while ice nucleation is included in some of the studies, the precipitation parameterizations in global and continental scale models do not explicitly account for the GCCN effects of large particles.

60 In this study we apply UCLALES-SALSA large eddy simulator (Tonttila et al., 2017, 2021) to explore what kind of birch pollen concentrations are required to impact precipitation in liquid and mixed phase clouds in local scale. We quantify the CCN, GCCN and INP effects of pollen and SPPs for a range of pollen concentrations and test the effect of different assumptions about SPP size distribution. The simulations allow us to quantify the fraction of pollen and SPPs that escape the boundary layer to free troposphere and can participate in long-range transport in different cloud conditions.

65 **2 Methods**

2.1 Model description

We used the UCLALES-SALSA large eddy simulator, that includes sectional representations of aerosols, liquid cloud droplets, raindrops and ice and simulates their interactions (Ahola et al., 2020; Tonttila et al., 2017, 2021). The version of UCLALES-SALSA used in this study explicitly computes rain drop formation through collision-coalescence of cloud droplets. This process is included in the collision scheme that handles all collisions between different types of particles including coagulation of aerosol particles, coalescence of cloud droplets, accretion of liquid droplets to ice particles and scavenging of aerosol and cloud droplets by falling raindrops or ice. The cloud droplets are moved to rain phase when their wet diameter after collision exceeds minimum drop size of 20 μm . When liquid droplets leave the cloud to subsaturated conditions and enough water evaporates to bring the particles close to equilibrium with the ambient relative humidity, they are moved back to aerosol phase.

75 The model was amended with parameterizations for pollen emission and humidity dependent rupture. Pollen is emitted as constant flux from surface. We simulate pollens as spherical particles, birch pollen with diameter of 22 μm and density of 800 kg/m^3 (Gregory, 1961) and pine pollen with diameter of 59 μm and density of 450 kg/m^3 (Jackson and Lyford, 1999). Direct emission of sub-pollen particles from trees is not considered in this study, as there is no data available to quantify such flux.

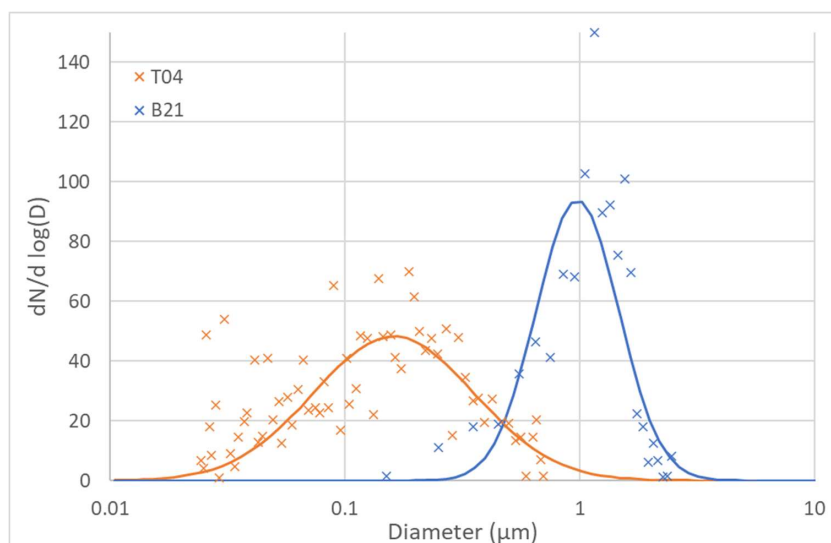
80 As no measurement data about humidity dependent pollen rupture rate is available for birch pollen, we followed the example of Werchner et al. (2022) and parameterized the rupture process as exponential decay with timescale and humidity dependence approximated from the data of Zhou, (2014) for wheat pollen. Pollens start rupturing when relative humidity exceeds 80% and their e-fold lifetime reduces linearly from 12.5 to 2.5 hours as humidity increases from 80% to 95%. We limit the e-fold lifetime to minimum half an hour. This exponential decay approximation would overestimate the rupture rate at the beginning of the Zhou's (2014) experiments where the temporal development is looking more sigmoidal, however, the slow starting rate in the lab could be due to using dry pollen, while in nature the pollens have been exposed to ambient humidity already in the catkins. Thus, given all the uncertainties, we selected to use the simplest form of parameterization. The mass of the rupturing pollens is reduced by the total mass of the released SPPs, after which they continue interacting with the clouds as GCCN and INP but are not allowed to rupture again. Pollens rupture much faster when fully immersed in water, as is the case when a



pollen is included in a raindrop. However, it is unclear if the released fragments would be able to leave the raindrop or they
 90 would stay inside the drop and stick to the surface of the pollen grain when the drop evaporates. For simplicity, we simulate
 no SPP release from raindrops and consider the pollens that have been in raindrops incapable of rupturing further.

The size of the SPPs affects their ability to act as both CCN and INP. To explore the impact of different assumptions regarding
 the size of the SPPs, lognormal distributions (Figure 1) were fitted to the measurements from Taylor et al., (2004) (mean
 diameter 0.3 μm , geometric standard deviation 2.2, referred as T04 further on) and Burkart et al., (2021) (mean diameter 1.15
 95 μm , geometric standard deviation 1.5, further referred as B21). Following Wozniak et al. (2018), we assumed 1000 sub-pollen
 particles to be emitted from each ruptured pollen, which is similar to assessments of Stone et al. (2021) and Suphioglu et al.
 (1992).

In addition to size and density, the cloud interactions are also sensitive to particle's hygroscopicity. We set the hygroscopicity
 parameter to 0.16 for both SPPs and whole pollens, which is consistent with the critical supersaturation measurements for
 100 birch pollen SPPs by Steiner et al. (2015). As a whole pollen is not a soluble particle, use of kappa-Koehler theory (Petters and
 Kreidenweis, 2007) is not exactly correct for it. However, as particles with diameters in the range of tens of micrometres
 activate easily as cloud droplets as long as they are not hydrophobic, this approximation should have limited impact.



105 **Figure 1: Size distributions fitted to data from Taylor et al., (2004) (orange) or Burkart et al., (2021) (blue).**

Ice nucleation parameterization for both pollen and sub-pollen particles was based on a simplified version of the Augustin et
 al. (2013) scheme. The temperature dependence of the ice nucleation rate is computed as an exponential fit: $j =$
 $2.32 \times 10^{-8} \times e^{-0.835 \times T_c}$ where j is the heterogeneous nucleation rate per second and T_c is the temperature in Celsius. We



110 account for the probability that a small SPP particle might not contain any ice-nucleation-active macromolecules, however, to
avoid unrealistically high ice nucleation rates for whole pollen grains in near-zero temperatures, we assume that there is exactly
one ice nucleation active site in every larger SPP and whole pollen. Augustin et al. (2013) showed in their Appendix A that
this approximation reproduces well the slope of the frozen fraction. For whole pollens it gives us a median freezing temperature
of ~ -15 °C at a cooling rate of 0.67 K per minute used by Gute and Abbatt (2020), which is slightly lower than their measured
115 median freezing temperature -13.4 °C but on the higher end of the rest of their reviewed data. The freezing rate in the model
is zeroed for temperatures above -2 °C. All particles formed by collisions with ice are assumed to freeze. Secondary ice
formation through rime splintering (Hallett and Mossop, 1974) is included in the simulations. Splinters are formed at
temperatures between -3 and -8 °C with 3.5×10^8 splinters produced per kilogram of rime at the optimal -5 °C temperature. The
parameterization of Seifert et al. (2014) for cloud ice is used for the effective size and terminal velocity of the ice particles.

120 2.2 Model simulations

To investigate the impact of high pollen concentrations to cloud processes, we simulate two well described cases – one for
liquid and one for mixed-phase clouds.

For liquid clouds we use the RICO Field Campaign characterized by lightly precipitating cumulus-topped boundary layer,
adapted for large eddy simulator (LES) studies by VanZanten et al. (2011), who selected the case as a simple prototype for
125 precipitating convective clouds. The clouds in this case are shallow enough to simulate with LES without the domain size
becoming computationally prohibitively expensive while still being deep enough for precipitation development, and sensitive
to microphysics including aerosol perturbations. The case allows us to investigate the role of convective structures in
transporting particles such as pollen and SPPs from boundary layer to the free troposphere where they can be transported for
long distances and contribute to cloud and ice nucleation processes in larger scale. The near surface temperature during the
130 campaign was $+26$ °C. Such high temperature on a spring day would result in rapid pollen maturing and release and thus would
lead to very high pollen concentrations. The temperature was above zero throughout the cloud layer.

For mixed phase clouds we use the second case described by (Calderón et al., 2022). The measurement campaign that their
LES simulations were based on took place in Puijo station, Finland. The case is characterized by a low-level stratocumulus
cloud with low aerosol loading and light drizzle formation in cloud. The near-surface temperature was about 0 °C and some ice
135 particles were observed. We extended the simulations to 24 hours from the original 6 hours to allow the pollen to be transported
to the cloud, rupture to produce SPPs, and ice nucleation to take place. The cloud top temperature at the beginning of the
episode was about -3 °C and was falling while the cloud top was rising. These temperatures are ideal for secondary ice
production through rime splintering (Hallett and Mossop, 1974). While high pollen emission is unlikely with near-zero
temperature, Puijo station is elevated compared to its surroundings where the temperature is likely to be higher. Also, the case
140 starts at midnight, so the pollen could have matured during the warmer afternoon while its release from catkins could have
been delayed due to too high humidity or low wind conditions. The case also gives us a chance to investigate if any pollen or
SPPs manages to escape the boundary layer through the relatively strong inversion that was present in this case.



In both cases the birch pollen emission flux was calibrated to produce near surface concentrations covering from commonly observed daily mean values of about 1000 up to the hourly maximum values of more than 50000 pollens per m³. Fluxes required in the simulations to produce these concentrations are shown in Table 1. Simulations with T04 SPP distribution were made only for the maximum pollen flux to save computational resources. To investigate the impact of pollen size to the GCCN effect, one extra simulation was made for the RICO case in which the pollen emission flux was kept the same as in the maximum birch pollen flux but pine pollen size and density were assigned. Pine pollen can be present in atmosphere in large quantities. Its diameter is about 3 times larger than that of birch pollen however, pine pollens incorporate two large air bladders that reduce its density and help with buoyancy. As Zhou, (2014) found no rupture for pine pollen, we do not consider this process for the pine pollen simulation.

The setup of the simulations is shown in Table 1. Both cases were run for 24 hours with 1 second internal timestep, which is further shortened if needed for model stability. Model spin-up allows the turbulence to develop while precipitation formation is turned off.

155

Table 1. Model setup

Cloud type	Liquid cumulus	Mixed-phase
Case reference	RICO, VanZanten et al. (2011)	Calderón et al. (2022)
Domain size	12.8 x 12.8 km	1.92 x 1.92 km
Horizontal resolution	80 m	30 m
Domain height	4 km	1.2 km
Vertical resolution	30m	10 m
Simulation length	24 h	24 h
Internal timestep	1 s	1 s
Output timestep	3 min	1 min
Spinup	2 h	1 h
Pollen emission calibration: surface flux and resulting near-surface concentration	30 #/m2/s -> 1340 #/m3 300 #/m2/s -> 13000 #/m3 1500 #/m2/s -> 60500 #/m3	50 #/m2/s -> 1180 #/m3 500 #/m2/s -> 11500 #/m3 2500 #/m2/s -> 56200 #/m3

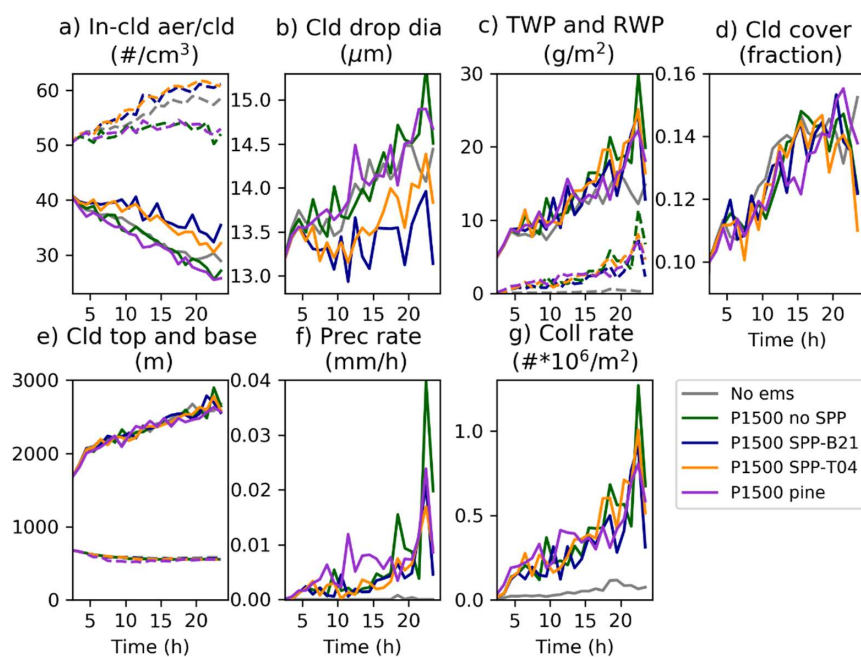


3 Results

3.1 Cumulus case

160 To investigate the impact of pollen and SPPs on liquid clouds we simulated the RICO Field Campaign characterized by cumulus-topped boundary layer, adapted for large eddy simulator studies by VanZanten et al. (2011). As seen from Figures 2-4, the UCLALES-SALSA simulation of this case without pollen emission produces almost no precipitation within 24 hours. Our results show no significant difference in cloud cover fraction and cloud height between the simulations with and without pollen (Figure 2d, e). However, the GCCN effect of the pollens enhances the collision-coalescence rate in the simulations and leads to increased surface precipitation (Figure 2f, g). The domain averaged accumulated precipitation is low even for the maximum emitted pollen flux; however, some isolated larger clouds can produce noticeable precipitation rates (Figure 3,A).

165



170 **Figure 2. Impact of pollen and SPPs on the clouds.** Panels: a – in-cloud interstitial aerosol (solid) and cloud droplet (dashed) concentration, b – cloud droplet size, mean over cloudy grid cells, c – total water path (solid) and rain water path (dashed), d – cloud fraction, e – height of cloud top (solid) and base (dashed), f – precipitation rate at surface, g – loss rate of cloud droplets due to collision-coalescence. Simulations: grey – no-emission control, green – birch pollen flux (1500 pollen/m²/s), no rupture, dark blue – same birch pollen flux, SPP size from B21, orange – same birch pollen flux, SPP size from T04, purple – pine pollen flux (1500 pollen/m²/s), no rupture. Hourly averaged time series, mean over the model area. Grid cell is considered cloudy if cloud water mixing ratio exceeds 1.e-5 kg/kg.

175



Panel B of Figure 3 shows the histograms of the instant precipitation rate in every grid-column every output timestep (3 minutes) of the second half of the simulations, when the pollen and SPPs had had time to start influencing the precipitation. As the cloud cover fraction stayed below 15% in all simulations, we can expect no rain in at least 85% of the domain. Indeed, precipitation stayed below 0.001 mm/h in more than 90 % of the domain in all simulations. As seen from Panel B of Figure 3, 180 the shapes of the rain rate distributions are very similar between all the simulations and increasing pollen emission increases the number of precipitating grid-cells in every rate interval. This indicates that the increase in accumulated precipitation is not due to heavier rainfall from a few clouds but due to larger fraction of the clouds precipitating.

The precipitation enhancement is nearly linear to the pollen emission (Figure 4, B). Including the pollen rupture process increases the cloud droplet number and reduces the cloud droplet size, stabilizing the clouds and decreasing the precipitation 185 (Figure 2, A, B). This effect is larger in the case of the B21 parameterization that assumes larger SPP size which allows larger fraction of SPPs to activate as cloud droplets.

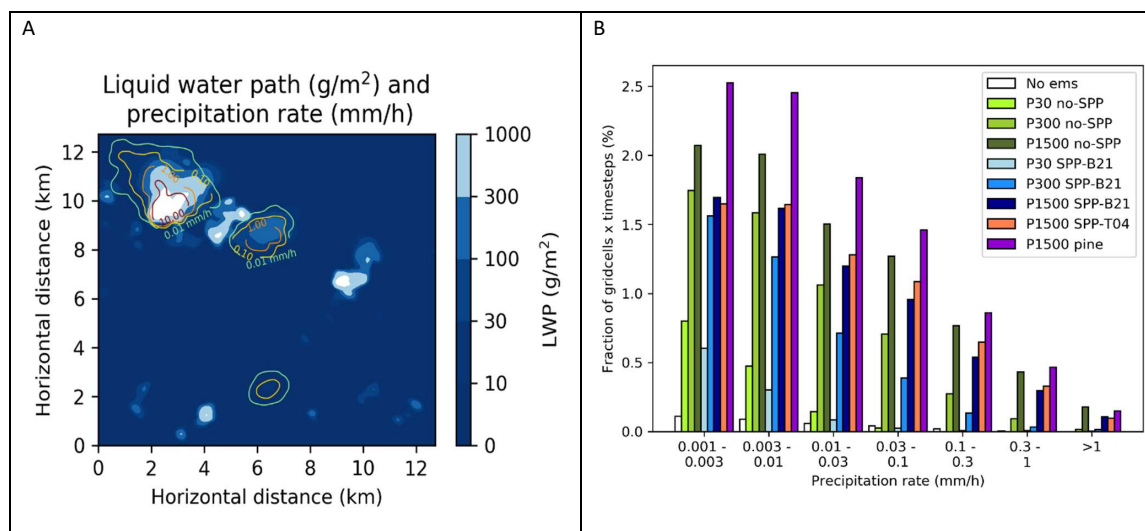


Figure 3. a) Contours – an example map of instant precipitation rate (mm/h), white shading –liquid water path (g/m²); b) histogram of instant grid cell rain rates in the second half of the simulation (mm/h). Precipitation rates below 0.001 mm/h are not shown.

190

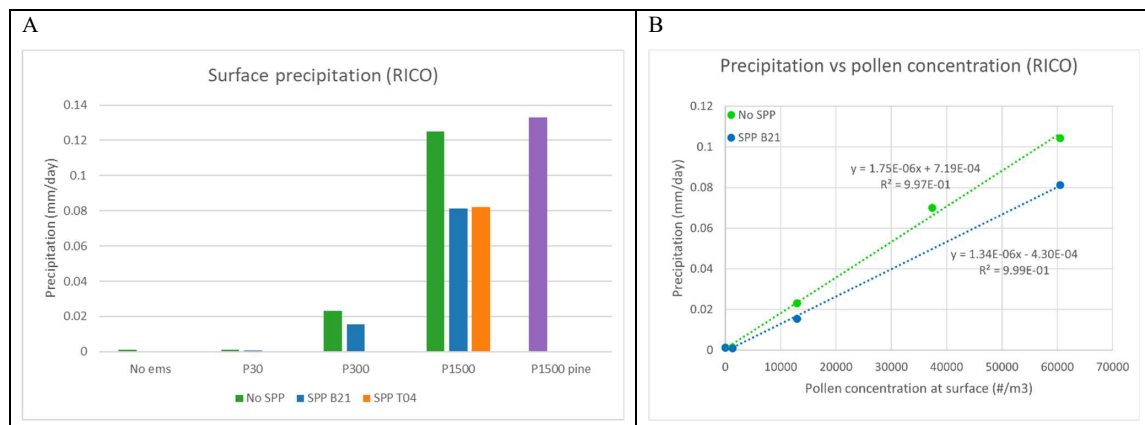


Figure 4. A – total accumulated surface precipitation by the end of the 24 hour simulations of RICO case with various emissions. B - Accumulated precipitation vs mean pollen concentration near surface at the second half of the simulation; blue – no rupture, blue (or orange) – SPP size distribution from B21 (or T04).

195

Figure 5 and Figure 6 show the vertical profiles of pollen and SPP number concentration and its tendencies in aerosol, cloud and rain phases caused by various processes in the midpoint of the simulation with maximum pollen emission and rupture according to B21 size distribution. Pollen is emitted from the surface and thus has a large vertical gradient near ground. Below cloud it is mostly in aerosol phase. Cloud activation takes place at the cloud base and above that the pollen-containing cloud droplets are quickly converted to raindrops.

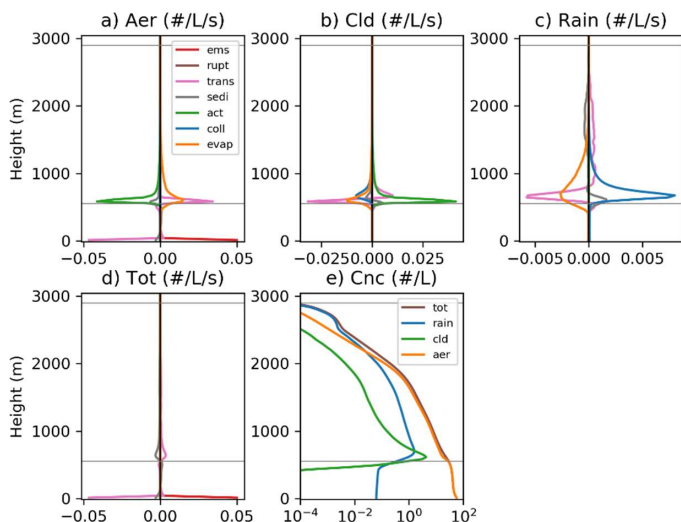
200

As seen from panel d of Figure 6, the most intense pollen rupture takes place at the cloud base where the humidity is high and pollen concentration is still reasonably high. Pollen rupture is not visible on Figure 5 because the ruptured pollens are still tracked in the simulation, so their number does not change. The produced fine sub-pollen particles are transported up or down and partly also immediately activated to cloud phase.

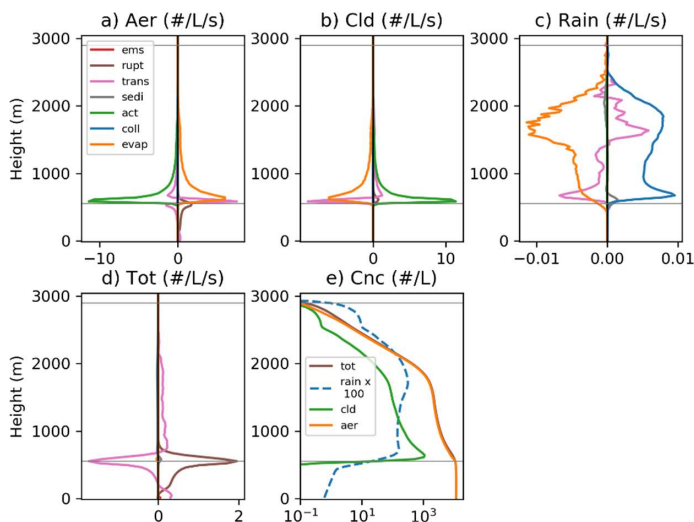
205

From Figure 6 panel c we see that smaller particles such as SPPs form raindrops more uniformly throughout the cloud layer, while pollen including raindrops (Figure 6, panels c and e) form mostly close to the cloud base. The raindrops formed around pollen grains are larger and thus fall faster and have less time to evaporate, leading to larger liquid water flux to surface, while large fraction of the SPP containing raindrops evaporates already on higher altitudes.

210



215 **Figure 5. Vertical profiles of pollen concentration tendencies in aerosol (A), cloud (B) and rain (C) phases, and the sum of those (D) due to various processes: pollen emission, rupture, vertical transport, sedimentation, cloud activation, collisions and evaporation. E – number concentration profiles of different phases. Domain averaged hourly mean quantities 12 hours after the beginning of the simulations, plotted for the case with maximum pollen flux and rupture according to B21 size distribution. Grey lines denote the cloud base and top of highest clouds. Both whole and ruptured pollen grains are included.**



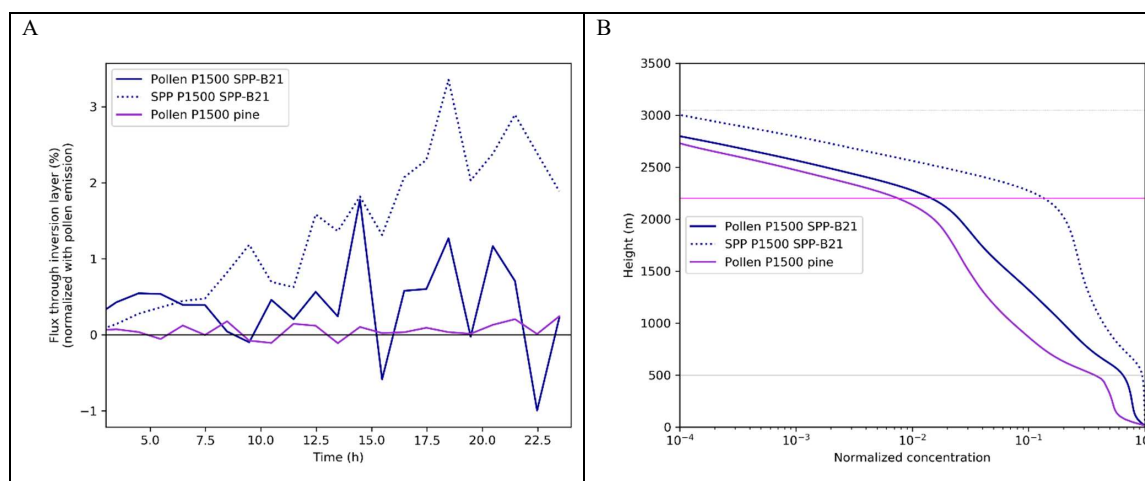
220 **Figure 6. A-D Vertical profiles of sub-pollen particle concentration tendencies in different phases due to various processes. Panels and colors same as in Figure 5. E – number concentration profiles of SPPs in different phases. Rain phase has been multiplied with factor of 100 to fit in the same scale.**



Pollen size has a two-fold effect on its ability to act as GCCN – on one hand large pollen would be more efficient in collecting cloud droplets to form precipitation but on the other hand the higher deposition rate of the larger particles would lead to much lower concentration at cloud level. For pine pollen the enhanced deposition resulted in three times lower near-ground concentration than for birch pollen and also faster drop off for higher vertical levels (Figure 7, B). However, the resulting precipitation started earlier (Figure 2,f) and was slightly larger than for the birch pollen case (purple bar on Figure 4).

225 Panel A of Figure 7 shows the normalized net flux of pine and birch pollens and birch SPPs through the inversion layer. The fluxes are positive for most of the simulation time, although for pine pollen the flux is very small. In the last hour of the simulation 0.03% of pine pollen, 0.14% of birch pollen and 1.86% of birch SPPs cumulatively emitted or produced during the whole simulation are located above the inversion layer. Majority of birch pollen and SPPs (88% and 98% respectively) above

230 the inversion layer are found in aerosol phase, indicating that they have escaped the clouds through detrainment. As SPPs survive higher in the cloud than pollens, more of them are released from the evaporating cloud droplets at higher altitudes (Figures 5 and 6 ,panels a-c). By the end of the simulation the number of SPPs above the inversion layer is 3 to 4 orders of magnitude higher than that of pollen.



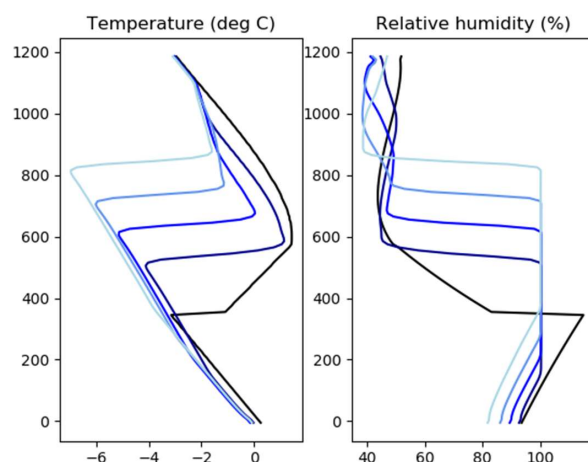
235 **Figure 7. A – Domain mean hourly averaged net flux of pollen and SPPs through the inversion layer. For pollen the flux is normalized with the pollen emission flux and for SPPs with pollen emission $\times 1000$. B – Normalized domain average vertical profiles of pollen concentration for birch (blue) and pine (purple) pollens and birch SPPs (blue, dashed) at the end of the simulation. The magenta line denotes the inversion layer, the solid gray the cloud base and the dashed gray the top of the highest clouds.**

3.2 Mixed phase case

240 For mixed phase clouds, we simulated the second case described by Calderón et al. (2022), a nocturnal low level stratocumulus episode observed in Puijo, Finland. In the course of the 24-hour simulation the cloud top rises from below 400 m to above 800



m and the cloud top temperature falls from -3 to -7 °C (Figure 8). Some snowflakes were observed during the measurement campaign but UCLALES-SALSA simulation without pollen emission produces almost no precipitation within 24 hours and as no INPs were included in the background aerosol, no ice is formed.

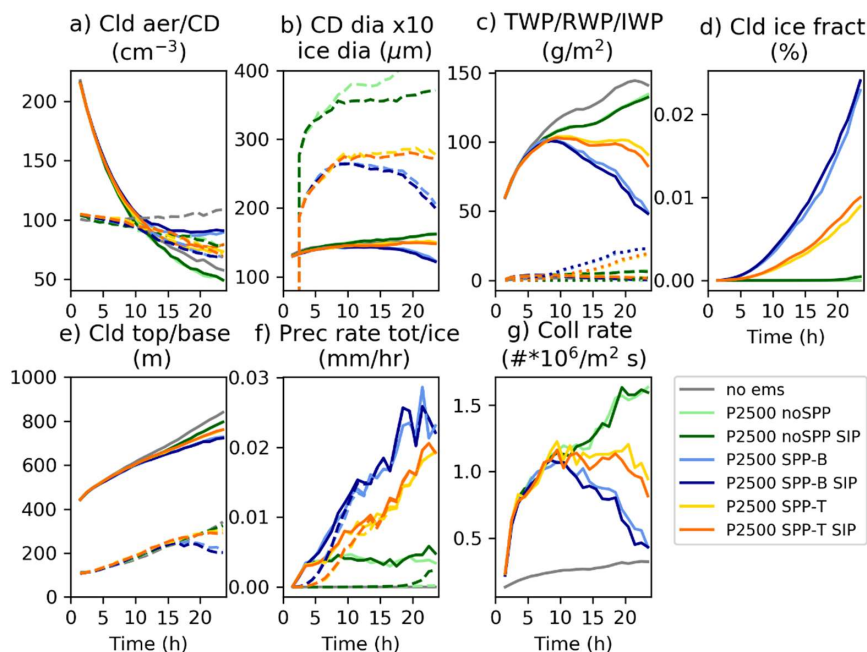


245

Figure 8. Horizontally averaged temperature and relative humidity profiles (initial, 6, 12, 18 and 24 hours after simulation start, from darker to lighter lines).

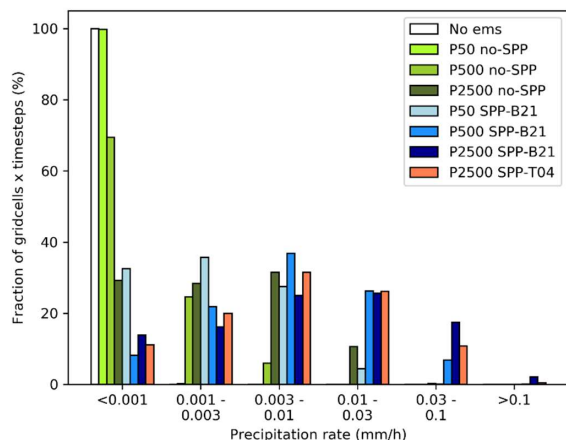
As seen from Figures 9-11, introduction of pollen to the simulations without the rupture process leads to light liquid phase drizzle due to the GCCN enhancing the collision rate, however, the pollen concentration in the clouds is too low to cause significant ice nucleation even for the maximum pollen flux. The rupture of a pollen grain produces 1000 potentially ice nucleating SPPs that also have slower settling velocity and thus their concentration in the cloud top can be much larger. As the relative humidity in this case was above 80% from surface to cloud top (Figure 8, right), the rupture rate of pollens was relatively fast. While these additional particles reduce the cloud droplet and ice particle size (Figure 9, b), they also make the cloud start to glaciate and lead to noticeable solid phase precipitation, especially if assuming the larger size distribution (B21), as according to the used ice nucleation parameterization, not all the smallest SPPs include ice nucleating macromolecules. For total precipitation, the large impact of additional INPs dominates over the competing effect of the extra CCN reducing cloud droplet size. As pollen rupture is a relatively slow process, it takes several hours for the SPP ice nucleation effect to start dominating over the pollen GCCN effect. Secondary ice production through rime splintering has minimal effect to the simulations (Figure 11 A), with the exception of the no-SPP case where the ice precipitation rate starts rising at the end of the simulation (Figure 9, panel f), indicating that the process could become important in longer timescale.

260



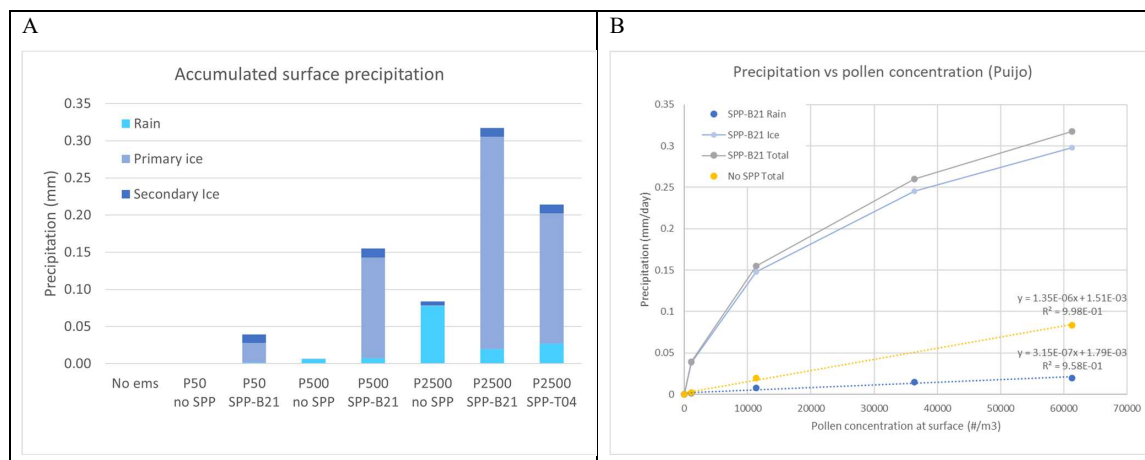
265 **Figure 9. Impact of pollen and SPPs on the clouds. Panels: a – in-cloud interstitial aerosol (solid) and cloud droplet (dashed) concentration, b –cloud droplet and ice particle size, mean over cloudy grid cells, cloud droplet diameter has been multiplied with 10 to fit on same scale, c –total water path (solid), rain water path (dashed) and ice water path (dotted), d -cloud ice fraction, e – height of cloud top (solid) and base (dashed), f –precipitation rate at surface, total (solid) and ice (dashed), g – loss rate of cloud droplets due to collision-coalescence Simulations: grey – no-emission control, green –birch pollen flux (2500 pollen/m²/s), no rupture, blue – same birch pollen flux, SPP size from B21, orange– same birch pollen flux, SPP size from T04. Darker shades indicate simulations that include secondary ice formation (SIP).**

In this case, the cloud cover is 100% in all simulations and precipitation is distributed uniformly over the model domain.
 270 During the second half of all the simulations with SPP release, and also the one with maximum pollen emission without SPP, light precipitation is present in majority of the domain. Higher INP concentration shifts the precipitation distribution towards higher rates (Figure 10). Similarly to the liquid cloud case, the resulting precipitation is positively correlated to pollen emission (Figure 11, right). Near-linear dependence is true for liquid precipitation while the solid phase levels off for higher INP concentrations.



275

Figure 10. Histogram of instant grid cell total precipitation (rain + ice) rates in the second half of the simulation (mm/h).



280

Figure 11. a - total accumulated surface precipitation (liquid and solid) by the end of the 24-hour simulations of Puijo case with various emissions. b - Scatter plot of precipitation vs pollen concentration near surface; yellow – no rupture, the rest – SPP from B21: gray - total precipitation, dark blue – rain, light blue - ice

Figure 12 and Figure 13 show the vertical profiles of aerosol and pollen number concentration tendencies in aerosol, cloud and rain and ice phases caused by various processes in the middle of the simulation with maximum pollen flux and rupture according to B21 size distribution.

285

Above the steep near-surface gradient the total pollen concentration in this case is much more uniform until the top of cloud layer (Figure 12, f), which is much lower than in the RICO case. Practically all pollens in rising airflows are activated to cloud



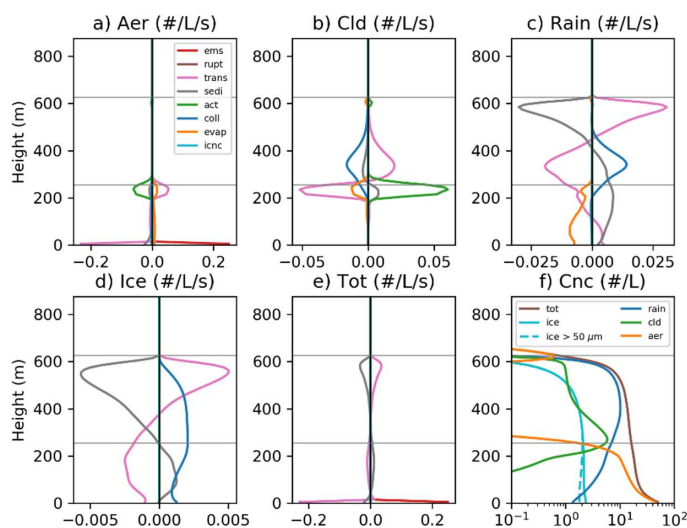
droplets at cloud base, followed by drizzle formation during the continuing ascent (Figure 12,a-c). Comparing the f panels of Figure 12 and Figure 13 shows that while part of the falling pollen-including raindrops do evaporate under the cloud base (Figure 12, c), the fraction of them reaching the ground is much larger than those with smaller core particles.

290 As seen from panels e and d on Figure 13, the ice nucleating SPPs are produced by pollen rupture near the cloud base and transported to the cloud top, where the temperatures are lowest and ice nucleation rate highest. The ice particles grow by deposition of water vapour while settling through the cloud layer. As the temperature is below zero at all vertical levels, they stay frozen until ground, but do shrink due to sublimation below cloud base. The role of whole pollen grains in ice nucleation is negligible due to their low concentration. Instead, as seen from panel d of Figure 12, they mostly end up in ice phase due to

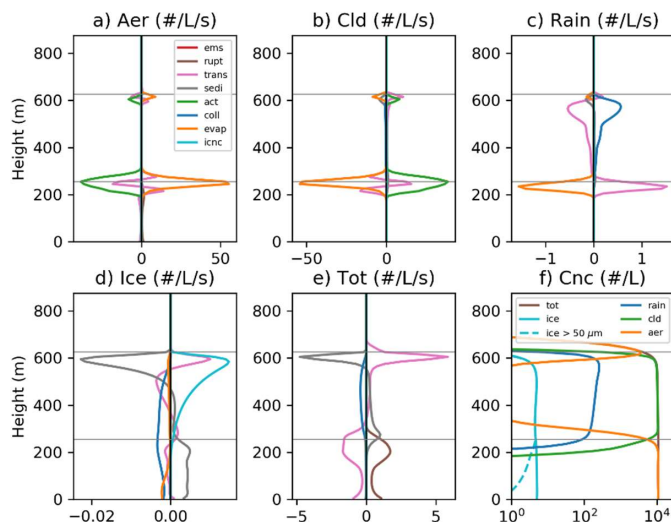
295 scavenging by falling ice particles. However, comparing solid and dashed light blue lines on Figure 12 and Figure 13 we see that after falling out of the cloud the majority of the SPP-containing ice particles shrink to small sizes due to sublimation, while the pollens have accumulated more water acting as GCCN even before freezing and thus fall faster and reach ground with larger water content, leading to increased ice-phase precipitation.

Although this case is characterized by a strong inversion, some particles still manage to escape above the cloud layer. By the

300 end of the 24-hour long simulation, 0.02% of the emitted pollen and 1.0% of the produced SPPs can be found above the cloud top. As seen from panels f of Figure 12 and Figure 13, above the clouds water has evaporated from pollen and SPPs and they have returned to aerosol phase - 70% of pollen and 87% of SPPs above the mean cloud top are found in aerosol phase.



305 **Figure 12.** Vertical profiles of pollen concentration tendencies in aerosol (A), cloud (B) and rain (C) and ice (D) phases, and the sum of those (E) due to various processes: pollen emission, rupture, vertical transport, sedimentation, cloud activation, collisions, evaporation, and ice nucleation. F – number concentration profiles of different phases. Dashed light blue line shows ice particles larger than 50 μm in diameter. Domain averaged hourly mean quantities 12 hours after the beginning of the simulations, plotted for the case with maximum pollen flux and rupture according to B21 size distribution. Grey lines denote the cloud base and top.



310

Figure 13. A-E Vertical profiles of sub-pollen particle concentration tendencies in different phases due to various processes, F – number concentration profiles of SPPs in different phases. Panels and colors same as in Figure 12.

4 Discussion and conclusions

We used the UCLALES-SALSA large eddy simulator for simulating pollen effects on precipitation in two well-described cases, one for liquid and one for mixed-phase clouds. The simulations showed that the effects of pollens and sub-pollen particles on precipitation could be noticeable in vicinity of birch or pine forests during the most intense pollination seasons, while more commonly encountered pollen concentrations are unlikely to cause a noticeable change. In both cases the liquid precipitation enhancement had nearly linear dependency on the emitted pollen flux, the slope of this relationship was case dependent. The ice precipitation from the mixed phase clouds levelled off for higher INP concentrations.

Although a small fraction of birch pollens managed to escape the boundary layer to the free troposphere, their impact is unlikely to extend far downwind from the source regions due to dilution and deposition reducing their concentration. Pine pollens are about trice larger than birch pollen but half as dense, leading to a few times higher settling velocity and shorter atmospheric lifetime. The fraction of pine pollens that got transported above the inversion layer by the updrafts in the convective clouds was about 5 times smaller than that of birch pollen. Thus, while more efficient as giant CCN, pine pollens are even less likely to be relevant to precipitation beyond the emission areas. However, the simulation with pine pollen led to slightly larger rain enhancement than birch pollen for same emission flux, showing that some of these extra-large particles managed to reach cloud level, and thus they could play a role in altering the precipitation for instance above the boreal forests.

The fine sub-pollen particles released when pollens rupture in humid conditions, on the other hand, have longer atmospheric lifetimes, having thus the potential to affect larger areas downwind the pollen emission. In our simulations around 1-2% of the



330 SPPs escaped boundary layer to free troposphere where they could accumulate and be transported for long distances to
contribute to INP population further downwind. By the end of the simulation the number of SPPs above the inversion layer
was up to 4 orders of magnitude higher than that of pollen. Zhang et al. (2024) reported a similar ratio of SPPs to pollen in
upper troposphere for their modelling study when using the same number of 1000 SPPs released from a rupturing pollen grain.
SPPs have two contrasting effects - while as extra CCN they slow down the precipitation formation, in mixed phase clouds
335 they also act as efficient high-temperature ice nucleators and can lead to formation of solid precipitation. Zhang et al. (2024)
found that the addition of SPPs also invigorated the deep convective system they studied as extra latent heat was released by
the enhanced cloud droplet formation. We did not observe this process in our liquid cumulus case as we saw no significant
differences in cloud top height or updraft velocities between the simulations with or without SPPs. The inclusion of SPPs lead
to diminished precipitation due to reduced collision-coalescence rate. In the mixed-phase cloud simulation the ice nucleation
340 by the SPPs clearly dominated over their cloud stabilizing effect and the total precipitation was increased.
While the relative effect of pollen on precipitation is likely the largest for clouds with very low precipitation like studied here,
the pollen could have larger overall impact on precipitation and cloud dynamics in different conditions than the simulated
cases, for instance in clouds more prone to precipitate or with lower CCN concentrations from other sources or with colder
cloud top temperature that would make the ice nucleation more efficient. SPP impacts of similar magnitude to the maximum
345 pollen emission cases would appear in lower pollen concentrations if more SPPs per rupturing pollen would be emitted, rupture
inside raindrops would release SPPs to air or SPPs would be directly emitted from trees. As observational data was not available
for birch pollen rupture humidity dependence and emitted SPP number, our model had to be based partly on data for other
wind-pollinated plants. Using the wheat pollen rupture data probably leads to overestimation of the rupture rate for birch. More
laboratory studies are needed to pin down these parameters.
350 The ice nucleation parameterization of Augustin et al. (2013) used in this study was based on measurements at temperatures
below -17 °C and thus its applicability for near-zero temperatures is uncertain. More laboratory studies are required to narrow
down this uncertainty. The measurements were made using pollen washing water and thus are also more valid for SPPs than
whole pollen grains. However, the pollen concentration at cloud top where majority of the ice nucleation happens never got
high enough to make noticeable impact on ice formation even when secondary ice formation through rime splintering was
355 accounted for.

Code availability

The source code of the version of UCLALES-SALSA used for the simulations can be found at <https://doi.org/10.57707/FMI-B2SHARE.5B37722CC31D4B8C9EDFECA6A8DD88F6> (Prank et al., 2024)



Data availability

360 The simulation data presented in this paper is available from <https://doi.org/10.57707/FMI-B2SHARE.5B37722CC31D4B8C9EDFECA6A8DD88F6> (Prank et al., 2024)

Author contribution

MP, SR and TR designed the study. MP performed and analysed the model simulations with assistance from JT, SR and TR. XS provided pollen observations and assisted with related literature. MP, JT, SR and TR have contributed to developing the
365 UCLALES-SALSA model. MP prepared the manuscript with contributions from all co-authors.

Competing interests

The authors declare that they have no conflict of interest.

Acknowledgements

This work was supported by the Academy of Finland projects 322532 and 356444.

370 References

- Ahola, J., Korhonen, H., Tonttila, J., Romakkaniemi, S., Kokkola, H. and Raatikainen, T.: Modelling mixed-phase clouds with the large-eddy model UCLALES-SALSA, *Atmos. Chem. Phys.*, 20(19), 11639–11654, doi:10.5194/acp-20-11639-2020, 2020.
- Augustin, S., Wex, H., Niedermeier, D., Pummer, B., Grothe, H., Hartmann, S., Tomsche, L., Clauss, T., Voigtländer, J.,
375 Ignatius, K. and Stratmann, F.: Immersion freezing of birch pollen washing water, *Atmos. Chem. Phys.*, 13(21), 10989–11003, doi:10.5194/acp-13-10989-2013, 2013.
- Burkart, J., Gratzl, J., Seifried, T., Bieber, P. and Grothe, H.: Subpollen particles (SPP) of birch as carriers of ice nucleating macromolecules, *Biogeosciences Discuss.*, 1–15, 2021.
- Calderón, S. M., Tonttila, J., Buchholz, A., Joutsensaari, J., Komppula, M., Leskinen, A., Hao, L., Moisseev, D., Pullinen, I.,
380 Tiitta, P., Xu, J., Virtanen, A., Kokkola, H. and Romakkaniemi, S.: Aerosol-stratocumulus interactions: Towards a better process understanding using closures between observations and large eddy simulations, *Atmos. Chem. Phys. Discuss.* [preprint], in review, doi:https://doi.org/10.5194/acp-2022-273, 2022.
- Dahl, Å., Galán, C., Hajkova, L., Pauling, A., Sikoparija, B., Smith, M. and Vokou, D.: The Onset, Course and Intensity of the Pollen Season, in *Allergenic Pollen*, edited by M. Sofiev and K.-C. Bergmann, pp. 29–70, Springer Netherlands,



- 385 Dordrecht., 2013.
- Dreischmeier, K., Budke, C., Wiehemeier, L., Kottke, T. and Koop, T.: Boreal pollen contain ice-nucleating as well as ice-binding “antifreeze” polysaccharides, *Sci. Rep.*, 7(October 2016), 1–13, doi:10.1038/srep41890, 2017.
- Duan, P., Hu, W., Wu, Z., Bi, K., Zhu, J. and Fu, P.: Ice nucleation activity of airborne pollen: A short review of results from laboratory experiments, *Atmos. Res.*, 285, 106659, doi:10.1016/j.atmosres.2023.106659, 2023.
- 390 Emmerson, K. M., Silver, J. D., Thatcher, M., Wain, A., Jones, P. J., Dowdy, A., Newbiggin, E. J., Picking, B. W., Choi, J., Ebert, E. and Bannister, T.: Atmospheric modelling of grass pollen rupturing mechanisms for thunderstorm asthma prediction, *PLoS One*, 16(4 April), 1–21, doi:10.1371/journal.pone.0249488, 2021.
- Gregory, P. H.: *The microbiology of the atmosphere*, edited by N. Polunin, Leonard Hill Books Limited / Interscience publishers, Inc., London / New York., 1961.
- 395 Gute, E. and Abbatt, J. P. D.: Ice nucleating behavior of different tree pollen in the immersion mode, *Atmos. Environ.*, 231(April), 117488, doi:10.1016/j.atmosenv.2020.117488, 2020.
- Gute, E., David, R. O., Kanji, Z. A. and Abbatt, J. P. D.: Ice Nucleation Ability of Tree Pollen Altered by Atmospheric Processing, *ACS Earth Sp. Chem.*, 4(12), 2312–2319, doi:10.1021/acsearthspacechem.0c00218, 2020.
- Hallett, J. and Mossop, S. C.: Production of secondary ice particles during the riming process., *Nature*, 249, 26–28, doi:https://doi.org/10.1038/249026a0, 1974.
- 400 Houghton, H. G.: Problems Connected with the Condensation and Precipitation Processes in the Atmosphere *, *Bull. Am. Meteorol. Soc.*, 19(4), 152–159, doi:10.1175/1520-0477-19.4.152, 1938.
- Jackson, S. T. and Lyford, M. E.: Pollen dispersal models in Quaternary plant ecology: Assumptions, parameters, and prescriptions, *Bot. Rev.*, 65(1), 39–75, doi:10.1007/BF02856557, 1999.
- 405 Petters, M. D. and Kreidenweis, S. M.: A single parameter representation of hygroscopic growth and cloud condensation nucleus activity, *Atmos. Chem. Phys.*, 7, 1961–1971, doi:https://doi.org/10.5194/acp-7-1961-2007, 2007.
- Prank, M., Tonttila, J., Shang, X., Romakkaniemi, S. and Raatikainen, T.: Data and code for the manuscript “Can pollen affect precipitation?” by Prank et al., , doi:10.57707/fmi-b2share.5b37722cc31d4b8c9edfeca6a8dd88f6, 2024.
- Ranta, H. and Satri, P.: Synchronized inter-annual fluctuation of flowering intensity affects the exposure to allergenic tree pollen in North Europe, *Grana*, 46(4), 274–284, doi:10.1080/00173130701653079, 2007.
- 410 Rantio-Lehtimäki, A., Viander, M. and Koivikko, A.: Airborne birch pollen antigens in different particle sizes, *Clin. Exp. Allergy*, 24(1), 23–28, doi:10.1111/j.1365-2222.1994.tb00912.x, 1994.
- Rantio-Lehtimäki, A., Helander, M. L. and Pessi, A. M.: Circadian periodicity of airborne pollen and spores; significance of sampling height, *Aerobiologia (Bologna)*, 7(2), 129–135, doi:10.1007/BF02270681, 1991.
- 415 Schäppi, G. F., Suphioglu, C., Taylor, P. E. and Knox, R. B.: Concentrations of the major birch tree allergen Bet v 1 in pollen and respirable fine particles in the atmosphere, *J. Allergy Clin. Immunol.*, 100(5), 656–661, doi:10.1016/S0091-6749(97)70170-2, 1997.
- Seifert, A., Blahak, U. and Buhr, R.: On the analytic approximation of bulk collision rates of non-spherical hydrometeors,



- Geosci. Model Dev., 7(2), 463–478, doi:10.5194/gmd-7-463-2014, 2014.
- 420 Skjøth, C. A., Šikoparija, B., Jäger, S. and EAN-Network: Pollen Sources, in Allergenic Pollen: A Review of the Production, Release, Distribution and Health Impacts, edited by M. Sofiev and K.-C. Bergmann, pp. 9–27, Springer Netherlands, Dordrecht., 2013.
- Steiner, A. L., Brooks, S. D., Deng, C., Thornton, D. C. O., Pendleton, M. W. and Bryant, V.: Pollen as atmospheric cloud condensation nuclei, *Geophys. Res. Lett.*, 42(9), 3596–3602, doi:10.1002/2015GL064060, 2015.
- 425 Stone, E. A., Mampage, C. B. A., Hughes, D. D. and Jones, L. M.: Airborne sub-pollen particles from rupturing giant ragweed pollen, *Aerobiologia (Bologna)*, 37(3), 625–632, doi:10.1007/s10453-021-09702-x, 2021.
- Suphioglu, C., Singh, M. B., Taylor, P., Knox, R. B., Bellomo, R., Holmes, P. and Puy, R.: Mechanism of grass-pollen-induced asthma, *Lancet*, 339(8793), 569–572, doi:10.1016/0140-6736(92)90864-Y, 1992.
- Taylor, P. E., Flagan, R. C., Miguel, A. G., Valenta, R. and Glovsky, M. M.: Birch pollen rupture and the release of aerosols of respirable allergens, *Clin. Exp. Allergy*, 34(10), 1591–1596, doi:10.1111/j.1365-2222.2004.02078.x, 2004.
- 430 Tonttila, J., Maalick, Z., Raatikainen, T., Kokkola, H., Kühn, T. and Romakkaniemi, S.: UCLALES-SALSA v1.0: A large-eddy model with interactive sectional microphysics for aerosol, clouds and precipitation, *Geosci. Model Dev.*, 10(1), 169–188, doi:10.5194/gmd-10-169-2017, 2017.
- Tonttila, J., Afzalifar, A., Kokkola, H., Raatikainen, T., Korhonen, H. and Romakkaniemi, S.: Precipitation enhancement in stratocumulus clouds through airborne seeding: Sensitivity analysis by UCLALES-SALSA, *Atmos. Chem. Phys.*, 21(2), 1035–1048, doi:10.5194/acp-21-1035-2021, 2021.
- 435 VanZanten, M. C., Stevens, B., Nuijens, L., Siebesma, A. P., Ackerman, A. S., Burnet, F., Cheng, A., Couvreux, F., Jiang, H., Khairoutdinov, M., Kogan, Y., Lewellen, D. C., Mechem, D., Nakamura, K., Noda, A., Shipway, B. J., Slawinska, J., Wang, S. and Wyszogrodzki, A.: Controls on precipitation and cloudiness in simulations of trade-wind cumulus as observed during RICO, *J. Adv. Model. Earth Syst.*, 3(2), doi:10.1029/2011MS000056, 2011.
- 440 Werchner, S., Gute, E., Hoose, C., Kottmeier, C., Pauling, A., Vogel, H. and Vogel, B.: When Do Subpollen Particles Become Relevant for Ice Nucleation Processes in Clouds?, *J. Geophys. Res. Atmos.*, 127(24), 1–14, doi:10.1029/2021JD036340, 2022.
- Wozniak, M. C., Solmon, F. and Steiner, A. L.: Pollen Rupture and Its Impact on Precipitation in Clean Continental Conditions, *Geophys. Res. Lett.*, 45(14), 7156–7164, doi:10.1029/2018GL077692, 2018.
- 445 Zhang, Y., Subba, T., Matthews, B. H., Pettersen, C., Brooks, S. D. and Steiner, A. L.: Effects of pollen on hydrometeors and precipitation in a convective system, *JGR Atmos.*, 129, e2023JD039891, doi:10.1029/2023JD039891, 2024.
- Zhou, Q.: Relative Humidity Induced Plant Pollen Grain Rupture and Conceptual Model Development, WASHINGTON STATE UNIVERSITY., 2014.